



THE UNIVERSITY *of* EDINBURGH

Edinburgh Research Explorer

Pravastatin ameliorates placental vascular defects, fetal growth, and cardiac function in a model of glucocorticoid excess

Citation for published version:

Wyrwoll, CS, Noble, J, Thomson, A, Tesic, D, Miller, MR, Rog-Zielinska, EA, Moran, CM, Seckl, JR, Chapman, KE & Holmes, MC 2016, 'Pravastatin ameliorates placental vascular defects, fetal growth, and cardiac function in a model of glucocorticoid excess', *Proceedings of the National Academy of Sciences*, vol. 113, no. 22, pp. 6265-70. <https://doi.org/10.1073/pnas.1520356113>

Digital Object Identifier (DOI):

[10.1073/pnas.1520356113](https://doi.org/10.1073/pnas.1520356113)

Link:

[Link to publication record in Edinburgh Research Explorer](#)

Document Version:

Peer reviewed version

Published In:

Proceedings of the National Academy of Sciences

Publisher Rights Statement:

Author's final peer-reviewed manuscript as accepted for publication.

General rights

Copyright for the publications made accessible via the Edinburgh Research Explorer is retained by the author(s) and / or other copyright owners and it is a condition of accessing these publications that users recognise and abide by the legal requirements associated with these rights.

Take down policy

The University of Edinburgh has made every reasonable effort to ensure that Edinburgh Research Explorer content complies with UK legislation. If you believe that the public display of this file breaches copyright please contact openaccess@ed.ac.uk providing details, and we will remove access to the work immediately and investigate your claim.



1 **PRAVASTATIN REVERSES PLACENTAL VASCULAR DEFECTS, RESTORES**
2 **FETAL GROWTH AND NORMALISES CARDIAC FUNCTION IN A MODEL OF**
3 **GLUCOCORTICOID EXCESS**

4
5 Caitlin S. Wyrwoll¹, June Noble², Adrian Thomson², Dijana Tesic¹, Mark R. Miller², Eva A.
6 Rog-Zielinska^{2,3}, Carmel M. Moran², Jonathan R. Seckl², Karen E. Chapman^{2, 1} and Megan C.
7 Holmes².

8
9
10

11 ¹School of Anatomy, Physiology & Human Biology, The University of Western Australia, 35
12 Stirling Hwy, Crawley, WA 6009, Australia.

13 ²University/BHF Centre for Cardiovascular Science, University of Edinburgh, Edinburgh
14 EH16 4TJ, United Kingdom.

15 ³Current address: National Heart & Lung Institute, Imperial College London, Middlesex, UB9
16 6JH, United Kingdom

17
18 **Corresponding author:** Caitlin Wyrwoll, School of Anatomy, Physiology & Human Biology,
19 The University of Western Australia, 35 Stirling Hwy, Crawley, WA 6009, Australia.

20 Email: caitlin.wyrwoll@uwa.edu.au.

21
22 Classification: BIOLOGICAL SCIENCES: Medical Sciences

23 Keywords: placenta, 11 β -HSD2, glucocorticoids, fetal heart

24 Short title: Pravastatin ameliorates feto-placental dysfunction

25
26
27

28 **ABSTRACT**

29 Feto-placental glucocorticoid overexposure is a significant mechanism underlying fetal growth
30 restriction and the programming of adverse health outcomes in the adult. Placental
31 glucocorticoid inactivation by 11 β -hydroxysteroid dehydrogenase type 2 (11 β -HSD2) plays a
32 key role. We previously discovered that *Hsd11b2*^{-/-} mice, lacking 11 β -HSD2, show marked
33 underdevelopment of the placental vasculature. We now explore the consequences for fetal
34 cardiovascular development and whether or not this is reversible. We studied *Hsd11b2*^{+/+},
35 *Hsd11b2*^{+/-} and *Hsd11b2*^{-/-} littermates from heterozygous (*Hsd11b*^{+/-}) matings at embryonic day
36 (E)14.5 and E17.5, where all three genotypes were present to control for maternal effects. Using
37 high-resolution ultrasound umbilical vein blood velocity in *Hsd11b2*^{-/-} fetuses did not undergo
38 the normal gestational increase seen in *Hsd11b2*^{+/+} littermates. Similarly, the resistance index
39 in the umbilical artery did not show the normal gestational decline. Surprisingly, given that
40 11 β -HSD2 absence is predicted to initiate early maturation, the E/A wave ratio was reduced at
41 E17.5 in *Hsd11b2*^{-/-} fetuses, suggesting impaired cardiac function. Pravastatin administration
42 from E6.5, which increases placental VEGFA and thus vascularization, increased placental
43 fetal capillary volume, ameliorated the aberrant umbilical cord velocity, normalized fetal
44 weight and improved the cardiac function of *Hsd11b2*^{-/-} fetuses. This improved cardiac function
45 occurred despite persisting indications of increased glucocorticoid exposure in the *Hsd11b2*^{-/-}
46 fetal heart. Thus, the pravastatin-induced enhancement of fetal capillaries within the placenta
47 and the resultant hemodynamic changes correspond with restored fetal cardiac function. Statins
48 may represent a useful therapeutic approach to intrauterine growth retardation due to placental
49 vascular hypofunction.

50 **SIGNIFICANCE STATEMENT:**

51 Environmental challenges *in utero* perturb fetal growth and alter subsequent adult health
52 outcomes. The role of the placenta is uncertain. We use a genetically modified mouse model of
53 feto-placental glucocorticoid excess which exhibits decreased placental vascularity and fetal
54 growth restriction. We show that this associates with retarded fetal heart development.
55 Strikingly, treatment with pravastatin restores placental vascularity and reverses retarded fetal
56 growth and cardiovascular development. These results highlight the potential of statins to
57 remedy placental vascular insufficiency and enhance fetal outcomes in compromised
58 pregnancy.

59 **INTRODUCTION**

60 Low birth weight is associated with an increased risk of cardiometabolic disorders in adulthood
61 (1). Frequently underlying this association is elevated fetal exposure to ‘stress hormones’ -
62 glucocorticoids. Endogenous glucocorticoids (cortisol in humans, corticosterone in rodents) are
63 a key signal in late gestation, which alter developmental trajectories of fetal tissues,
64 predominantly from a proliferative to differentiated state, in preparation for extra-uterine life
65 (2). Fetal overexposure to glucocorticoids in humans, primates and rodents is detrimental for
66 placental and fetal growth and development, and ‘programs’ higher risk of cardiometabolic
67 disease in later life (3-8). Recent data suggest that the detrimental effects of excess
68 glucocorticoids on fetal growth and development result from direct glucocorticoid actions on
69 the placenta as well as on the fetus itself (9, 10).

70
71 The fetus and the placenta are maintained in a low glucocorticoid environment by the abundant
72 expression of feto-placental 11 β -hydroxysteroid dehydrogenase-2 (11 β -HSD2), an enzyme
73 which inactivates the much higher levels of glucocorticoids arriving from the maternal
74 circulation (11, 12). In humans and in animal models, placental 11 β -HSD2 expression is
75 reduced in adverse situations including poor maternal nutrition or maternal stress (13-15).
76 Bypass of this protective enzyme, be it through synthetic glucocorticoids which are poor
77 substrates (9, 16), inhibition (by liquorice) or genetic ablation of *Hsd11b2* which encodes 11 β -
78 HSD2 (10), reduces placental weight. This is accompanied by reduced fetal capillary volume,
79 surface area density, length and diameter in the placental labyrinth zone. Underlying these
80 placental changes is a striking reduction in placental expression of vascular endothelial growth
81 factor (VEGF)-A (9, 10) a major driver of placental angiogenesis.

82
83 Recent evidence suggests that altered placental function, including its haemodynamics, has a
84 direct impact on the development of fetal organs, particularly the heart (17-22). If compromised
85 placental vascular development due to glucocorticoid excess can be rescued, this raises the
86 possibility of a treatment for adverse effects of placental dysfunction upon the fetal heart and
87 circulation. We therefore assessed placental and umbilical blood velocity and heart growth and
88 function in *Hsd11b2*^{-/-} fetuses and then took advantage of the placental VEGF-releasing effects
89 of pravastatin (23) to determine whether it might rescue or ameliorate the effects of fetal
90 glucocorticoid over-exposure.

91

92 **RESULTS**

93 ***Hsd11b2*^{-/-} fetuses fail to show the normal gestational maturation in umbilical cord blood**
94 **velocity and fetal heart function.**

95 To evaluate maturational changes in umbilical cord blood velocity and heart function, fetuses
96 of all 3 genotypes from male and female *Hsd11b2*^{+/-} matings underwent ultrasound analyses at
97 E14.5 (maximum of labyrinth zone 11 β -HSD2 expression (11, 12) and before fetal adrenal
98 gland steroidogenesis starts (24)), and at E17.5, (as placental 11 β -HSD2 falls, around peak fetal
99 plasma glucocorticoid levels, and just prior to birth, typically E18.5 in *Hsd11b2*^{+/-} mice (10)).
100 Umbilical vein blood velocity normally increases over gestation, as exemplified by the 1.4-fold
101 increase between E14.5 and E17.5 in wild type (*Hsd11b2*^{+/+}) fetuses (Fig 1A). Although not
102 different from control littermates at E14.5, umbilical vein blood velocity in *Hsd11b2*^{-/-} fetuses
103 did not undergo the normal gestational increase, such that by E17.5 umbilical vein blood
104 velocity was 24% less than wild-type (Fig 1A). Similarly, the normal gestation decline in
105 umbilical artery resistance (Resistance Index; RI=systole/[systole+diastole]), apparent in
106 *Hsd11b2*^{+/+} and *Hsd11b2*^{+/-} fetuses (18% decrease between E14.5 and E17.5) did not occur in
107 *Hsd11b2*^{-/-} fetuses (Fig 1B). Thus, there was an interaction between gestational age and
108 genotype for both umbilical vein blood velocity and RI. Heart function matures between E14.5
109 and E17.5, and as the fetal heart becomes more compliant, left ventricle (LV) filling becomes
110 more dependent on passive filling (the E wave) and less dependent on LV filling due to active
111 contraction of the atria (the A wave) (25). This clearly occurs in both *Hsd11b2*^{+/+} and
112 *Hsd11b2*^{+/-} fetuses but did not occur in *Hsd11b2*^{-/-} fetal hearts (Fig 1C). In contrast, myocardial
113 performance index, a combined measure of systolic and diastolic function (25), was unaltered
114 by genotype (see Table S1 for myocardial performance index and a breakdown of each of the
115 cardiac components assessed by ultrasound).

116

117 These functional changes were not due to altered gross morphology of the heart. Thus at E17.5
118 there were no differences in overall cardiac volume (*Hsd11b2*^{+/+}: 3.9 \pm 0.1, *Hsd11b2*^{+/-}: 3.8 \pm 0.2,
119 *Hsd11b2*^{-/-}: 3.4 \pm 0.3 mm³) or number of cardiomyocytes (*Hsd11b2*^{+/+}: 4.1 \pm 0.3, *Hsd11b2*^{+/-}:
120 4.1 \pm 0.2, *Hsd11b2*^{-/-}: 3.8 \pm 0.1 \times 10⁶). Perhaps analogously, cardiac function is altered in the
121 absence of gross morphological alteration in mice with cardiomyocyte and vascular smooth
122 muscle-specific deletion of the glucocorticoid receptor (GR) (26).

123

124 Altered blood velocity in the *Hsd11b2*^{-/-} umbilical cord prompted us to explore whether this
125 could be attributed to altered umbilical cord structure or function. Histology revealed no
126 significant differences between *Hsd11b2*^{+/+} and *Hsd11b2*^{-/-} in luminal area or wall thickness of
127 the umbilical artery or vein (Table S2). Functionally, isolated umbilical arteries from *Hsd11b2*^{-/-}
128 mice tended to be more responsive to vasoconstrictors and have lower basal release of
129 endothelium-dependent mediators. With loss of *Hsd11b2* there was no significant alteration in
130 maximal contractile response to high potassium (Fig 2B) while the thromboxane agonist,
131 U46619 reduced maximal contractile response (Fig 2C). The maximal contraction (K_{max}) to

132 U46619 was significantly lower in vessels from *Hsd11b2*^{-/-} compared to controls (2.41±0.24
133 mN vs 3.61±0.45 mN, respectively), although the sensitivity to U46619 (EC₅₀) did not differ
134 between genotypes. Basal endothelial function (basal release of nitric oxide and prostacyclin)
135 was explored through contractile response to L-NAME and indomethacin in the presence of an
136 EC₅₀ dose of U46619. L-NAME + indomethacin caused a further 25-50% transient contraction
137 of vessels ~ 2 min after addition, returning to baseline with 5 min (Fig 2D). The contractile
138 response was greatest in the umbilical arteries from control fetuses and lowest in arteries from
139 *Hsd11b2*^{-/-} (19±2% vs ±39±7%, p<0.05). Acetylcholine, an endothelium-dependent
140 vasodilator, did not relax umbilical arteries (Fig S1). The ability of umbilical arteries to relax
141 to other vasodilators was confirmed by a concentration-dependent relaxation response to the
142 nitric oxide donor drug, sodium nitroprusside (Fig 2E), with no differences in response between
143 genotypes. This pattern of response concurs with the *in vivo* findings. While increased umbilical
144 artery vasoconstriction and reduced endothelium-dependent functions likely contribute to
145 reduced fetal blood supply in 11β-HSD2 null fetuses, the differences between genotypes and
146 magnitude of the changes were modest and other factors are likely also to be involved (ie.
147 vascular resistance).

148

149 **Gene expression patterns in *Hsd11b2*^{-/-} fetal hearts reflect glucocorticoid overexposure**
150 **and earlier maturation.**

151 To investigate glucocorticoid exposure and probe mechanism underlying altered cardiac
152 function in *Hsd11b2*^{-/-} fetuses, we measured levels of mRNA encoding glucocorticoid-
153 responsive genes as well as genes important for contractile function. Cardiac expression of
154 *Tsc22d3* (also known as glucocorticoid-induced leucine zipper; GILZ, a mediator of anti-
155 inflammatory and perhaps other glucocorticoid actions) expression exhibited a normal
156 gestational increase (26) in *Hsd11b2*^{+/+} and *Hsd11b2*^{+/-} fetuses (Fig 3A). *Hsd11b2*^{-/-} fetuses
157 (gestational age and genotype interaction,) had elevated levels at E14.5, consistent with higher
158 glucocorticoid exposure in mid-gestation. Expression of *Myh6* (encoding myosin heavy chain-
159 α, MYHCα, the major contractile protein in the adult heart) normally increases between E14.5
160 and E17.5 (26), as exemplified by the 1.7-fold increase between E14.5 and E17.5 in *Hsd11b2*^{+/+}
161 and *Hsd11b2*^{+/-} fetal hearts (Fig 3B). While this gestational increase was exaggerated in
162 *Hsd11b2*^{-/-} fetuses, *Myh6* mRNA levels reduced (58%) at E14.5 and increased 1.4-fold at E17.5
163 compared with *Hsd11b2*^{+/+} littermates (Fig 3B). A similar pattern of expression was observed
164 for the *Atp2a2* gene encoding the calcium-handling protein SERCA2a (Fig 3C). The
165 downregulation of both *Myh6* and *SERCA2a* genes at E14.5 appears at variance with higher
166 glucocorticoid exposure of *Hsd11b2*^{-/-} fetuses, predicted to cause early cardiac maturation. This
167 raises the possibilities that either premature glucocorticoid exposure fails to mimic the normal
168 maturational effects of glucocorticoids upon the heart, or that indirect dysmaturational effects

169 predominate. Secretion of cardiac natriuretic peptide A (ANP; encoded by *Nppa*) is stimulated
170 by stretch of the myocardium (27) and is considered a marker of cardiomyocyte hypertrophy
171 (28). Its expression increases with gestation, as apparent in *Hsd11b2^{+/+}* fetuses (1.8 fold
172 between E14.5 and E17.5, Fig 3D). However, neither *Hsd11b2^{-/-}* nor *Hsd11b2^{+/-}* fetuses showed
173 this developmental increase in ANP expression in the heart. This suggests the *Hsd11b2^{-/-}* fetal
174 heart tissue is less compliant, as shown by ultrasound *in vivo*. Thus, overall *Hsd11b2^{-/-}* fetuses
175 show complex, gene-specific patterns of premature, exaggerated or reversed maturation of
176 glucocorticoid-sensitive transcripts in the myocardium.

177

178 **Pravastatin increases labyrinth zone *Vegfa* expression and fetal capillary volume in all** 179 **genotypes**

180 To determine if the adverse effects of glucocorticoid overexposure on the placental vasculature
181 can be overcome and whether this might beneficially impact on fetal heart development, we
182 administered (i.p.) either pravastatin or saline from E6.5 onwards with the aim of stimulating
183 placental VEGFA production and thereby enhancing vascularization. Consistent with its
184 reported effects on placental VEGF (23), pravastatin up-regulated expression of labyrinth zone
185 *Vegfa* in all genotypes (Fig 4A). The increase in *Hsd11b2^{-/-}* placentas was greater (genotype x
186 treatment), eliminating the genotype difference in placental *Vegfa* expression. Despite its role
187 in regulating *Vegfa* expression (29), labyrinth zone *Pparg* expression levels did not correspond
188 with *Vegfa* patterns (Figure 4B); pravastatin had no effect on *Pparg* mRNA expression and a
189 reduction in *Pparg* mRNA was apparent in both saline and pravastatin-treated *Hsd11b2^{-/-}*
190 placentas.

191

192 Corresponding with increased placental *Vegfa*, placental weight increased with pravastatin
193 (Table 1). Stereological assessment of labyrinth zone volume showed that while *Hsd11b2^{-/-}*
194 saline treated placentas appeared smaller this was not statistically significant (Fig 4C).
195 Furthermore, there was only a trend (p=0.0536) for labyrinth zone volume increase with
196 pravastatin (Fig 4C). Detailed investigation of fetal capillary volume provided a clearer insight
197 into placental vascular development. Thus, pravastatin modestly increased the volume of fetal
198 capillaries within the labyrinth zone of *Hsd11b2^{+/+}* and *Hsd11b2^{+/-}* fetuses (Fig 4D) but
199 completely rescued the deficit in *Hsd11b2^{-/-}* placentas, with a significant interaction between
200 treatment and genotype. There were no effects of pravastatin on maternal body weight, organ
201 weight or litter size (Table S3).

202

203 **Pravastatin strikingly attenuates fetal growth restriction and reverses adverse umbilical** 204 **flow and cardiac function in the *Hsd11b2^{-/-}* placenta and fetus.**

205 In saline-treated pregnancies, *Hsd11b2*^{-/-} fetuses were lighter than littermate controls as
206 previously reported (10) (Table 1). Pravastatin treatment increased fetal weight across all
207 genotypes, though *Hsd11b2*^{-/-} remained lighter than their *Hsd11b2*^{+/+} and *Hsd11b2*^{+/-}
208 littermates (Table 1). However, pravastatin ameliorated the growth retardation in *Hsd11b2*^{-/-}
209 fetuses such that they were the same weight as *Hsd11b2*^{+/+} controls.

210

211 Pravastatin had a marked effect on placental blood velocity and fetal heart measures. Overall,
212 pravastatin increased umbilical vein blood velocity (Fig 5A), decreased umbilical artery
213 resistance index (Fig 5B) and increased fetal cardiac E/A wave ratio (Fig 5C) in all genotypes.
214 Notably, pravastatin ‘normalised’ the aberrant phenotype of *Hsd11b2*^{-/-} fetuses such that there
215 were no genotype differences in umbilical vein blood velocity or fetal cardiac E/A ratio in
216 *Hsd11b2*^{-/-} fetuses from pravastatin-treated dams (Fig 5A and C). In contrast, the resistance
217 index remained increased in both saline-treated and pravastatin-treated *Hsd11b2*^{-/-} fetuses albeit
218 to a lesser extent in the pravastatin-treated *Hsd11b2*^{-/-} fetuses compared to saline treated (Fig
219 5B).

220

221 The effects of pravastatin on cardiac functional changes were not accompanied by gross
222 morphological changes. Thus, there were no differences in overall cardiac volume, ventricular
223 lumen volume or the ratio of ventricular wall thickness to lumen volume (Table S5).

224

225 **Pravastatin markedly alters fetal cardiac *Ace* and some collagen mRNAs**

226 Expression of glucocorticoid-responsive *Tsc22d3* mRNA was not altered by pravastatin (Fig
227 6A), consistent with increased glucocorticoid exposure and reflecting similar findings from the
228 initial untreated cohort at E17.5 (Fig 3A). Therefore, the alterations in *Hsd11b2*^{-/-} fetal heart
229 function are likely independent of direct cardiac glucocorticoid action. Similarly, expression of
230 *Mhyc6* and *Atp2a2* were unaffected by pravastatin in all genotypes (Fig 6B and C). While there
231 was no effect of pravastatin on cardiac *Nppa* expression in *Hsd11b2*^{+/+} fetuses (Fig 6D), it
232 increased in pravastatin-treated *Hsd11b2*^{-/-} and *Hsd11b2*^{+/-} fetuses. Thus, pravastatin- rescued
233 cardiac *Nppa* expression in *Hsd11b2*^{+/-} and partially rescued *Hsd11b2*^{-/-} fetuses. Expression of
234 *Ace* was decreased in fetal hearts of all genotypes with pravastatin (Fig 6E) abolishing the
235 genotype difference seen in saline-treated fetuses.

236 Collagen is a key contributor to cardiac wall stiffness. In fetuses from saline-treated dams, there
237 was an increase in the cardiac expression of *Coll1a1* (which determines rigidity (30)) in
238 *Hsd11b2*^{-/-} and *Hsd11b2*^{+/-} fetuses, compared to *Hsd11b2*^{+/+} littermates (Fig 6F). This
239 difference was not evident in fetuses from pravastatin-treated dams. *Col3a1* (which determines
240 elasticity (30)) showed a reciprocal effect; *Col3a1* mRNA levels were reduced in hearts of
241 saline-treated *Hsd11b2*^{-/-} and *Hsd11b2*^{+/-} fetuses compared to wild-type littermates (Fig 6G).

242 However, whilst pravastatin had no effect in *Hsd11b2*^{+/+}, it increased *Col3a1* mRNA levels in
243 *Hsd11b2*^{-/-} and *Hsd11b2*^{+/-} fetuses. These expression patterns correspond with the changes in
244 cardiac function. For *Col4a1* (Figure 6H) there was no effect of genotype or treatment, but a
245 significant interaction. Thus, pravastatin increased *Col4a1* expression in hearts of *Hsd11b2*^{+/-}
246 fetuses by 8.5-fold, but decreased it in *Hsd11b2*^{-/-} fetuses (68% decrease). Pravastatin did not
247 alter *Vegfa* and *Pparg* in the fetal heart. These data demonstrate that while pravastatin does not
248 reverse cardiac glucocorticoid overexposure in *Hsd11b2*^{-/-} fetuses, it does change key collagens
249 and other endocrine genes in a pattern which corresponds with enhancement of *Hsd11b2*^{-/-} fetal
250 heart function.

251

252 **DISCUSSION**

253 Pravastatin treatment dramatically ameliorates the adverse phenotype of *Hsd11b2*^{-/-} fetuses;
254 placental labyrinth zone morphology, umbilical blood velocity, fetal weight and fetal heart
255 function and gene expression are, for the most part, normalised. Thus, despite persistently
256 increased placental and fetal glucocorticoid exposure in *Hsd11b2*^{-/-} fetuses it is possible to
257 counter these adverse outcomes, including the “intra-uterine growth restriction” (IUGR)
258 phenotype. These findings highlight the crucial role of the placenta in informing fetal
259 development and suggest statins as a potential therapy for IUGR with placental vascular
260 insufficiency.

261

262 Despite the ‘maturation’ effects of antenatal glucocorticoids we surprisingly found that
263 *Hsd11b2*^{-/-} fetuses exhibit delayed or impaired cardiac functional maturation. Whether these
264 changes in fetal heart function alter cardiac function in adulthood will be important to uncover
265 in the future, though in this experimental model adult heart function is likely to be influenced
266 by the effect of life-long absence of 11 β -HSD2 upon salt regulation, blood pressure and renal
267 function (31), confounding interpretation. Pravastatin treatment then eradicated the impaired
268 *Hsd11b2*^{-/-} fetal cardiac maturation in conjunction with normalizing placental vascular
269 parameters. We postulate that placental and umbilical cord haemodynamics could be an
270 important factor directly influencing fetal heart development. Intervention is required to
271 demonstrate this. However, recent evidence supports the view that the placenta directly
272 influences the development of specific fetal organs, notably the heart. Thus, human placental
273 size and shape are epidemiologically associated with the incidence of cardiovascular disease in
274 later life (17, 32, 33). Thornburg et al. proposed (34) that because the fetal heart beats directly
275 against the resistance of the placental bed, changes in placental blood velocity must impact on
276 fetal heart development. Placental insufficiency (albeit severe – with absent or reversed
277 diastolic velocity in the umbilical artery) results in increased loading of the right ventricle (19).
278 Importantly, extensive work in genetically modified mouse models has revealed the necessity

279 of a functional placenta for optimal heart development; the cardiac defects exhibited in *Pparγ*
280 and *p38α* null embryos are rectified by targeted placental normalisation (21, 22, 35).
281 Furthermore, mice with genetic disruption of HOXA13, which is not expressed in the heart but
282 is an important transcriptional regulator of placental *Tie2* (and thus placental vascular
283 branching) show abnormal placental endothelium which is associated with reduced ventricular
284 wall thickness in the fetal heart (20), presumably occurring secondarily to the placental defect.

285

286 Pravastatin, an HMG-CoA reductase inhibitor which reduces cholesterol biosynthesis, is
287 currently contraindicated in pregnancy. This is due to its potential effects in altering NO
288 bioavailability in the fetal circulation, with detrimental consequences for the fetal brain sparing
289 response to acute hypoxia, as may happen intra-partum (38). However, pravastatin in various
290 mouse models of preeclampsia appears to ameliorate preeclamptic pathology (23, 39), and
291 pravastatin is currently the subject of a randomized control trial to ameliorate severe
292 preeclampsia (40). Three biological compartments are exposed to pravastatin in our model: 1)
293 the maternal, although our experimental design controls for alteration in maternal physiology
294 as all fetal genotypes are generated within the one pregnancy, 2) the placental and 3), the fetal.
295 Restoration of vasculogenesis in preeclamptic placentas following pravastatin has been
296 variously attributed to stimulation of placental VEGF release, soluble Flt-1 (sFlt-1; a VEGF
297 receptor), and placental growth factor (39, 41). Here, pravastatin enhanced labyrinth zone *Vegfa*
298 expression in all genotypes. Accordingly, fetal capillary volume, umbilical vein velocity and
299 umbilical resistance index underwent corresponding changes. Pravastatin will doubtless have
300 placental actions beyond *Vegfa*. Indeed in human first trimester placental explants, pravastatin
301 inhibits insulin-like growth factor 1 receptor function with adverse implications for trophoblast
302 differentiation (42). With regard to the fetus, the levels of pravastatin achieved within the fetal
303 circulation in this current study are unknown but earlier studies have demonstrated that transfer
304 of pravastatin in *ex vivo* human placenta does occur albeit to a limited extent (43, 44). However,
305 it is of interest to note that we observed no induction of *Vegfa* expression in *Hsd11b2*^{-/-} fetal
306 heart, suggesting that if pravastatin is eliciting direct effects on the fetus it may be via different
307 pathways. Whilst we cannot discount the potential for direct effects of pravastatin on the fetus,
308 the intriguing possibility is thus raised that the changes in cardiac parameters are primarily *due*
309 *to effects of pravastatin on enhancing the placental vasculature*, with effects on the fetal heart
310 occurring secondarily.

311

312 Further specific investigations are required to dissect this potential placenta-cardiac axis.
313 Placenta-specific removal of *Hsd11b2* and manipulation of VEGFA specifically in the placenta
314 will be useful to determine how placental vasculature impacts on fetal heart development and
315 function. Nevertheless, our findings suggest the intriguing possibility that using extrinsic

316 factors to enhance placental vasculature in compromised pregnancies could have beneficial
317 impact on fetal heart development and in IUGR more generally. Indeed, other gestational
318 insults, such as fetal hypoxia, which also cause IUGR and cardiovascular programming can be
319 overcome by administration of vitamin C (36, 37). However, the mechanism is likely different;
320 while oxidative stress was attenuated by vitamin C, placental labyrinth zone volume remained
321 unaltered (36, 37).

322

323 Overall, these data add to the growing body of evidence that placental vasculature has a key
324 role in fetal development and programming outcomes. Moreover, enhancement of placental
325 vasculature in compromised pregnancies may be beneficial for fetal heart development and in
326 IUGR.

327

328

329 **METHODS**

330 **Animals**

331 Male and female *Hsd11b2*^{+/-} mice, congenic on the C57BL/6J background (45), were mated
332 overnight and the morning of the day the vaginal plug was identified was designated E0.5. The
333 resultant pregnancies were only analysed if each of the possible offspring genotypes was
334 represented in the litter: *Hsd11b2*^{+/+} (“control” littermates), *Hsd11b2*^{+/-} and *Hsd11b2*^{-/-}. This
335 approach controls for alteration in maternal physiology as all fetal genotypes are generated
336 within the one pregnancy. Animals were given standard chow, water and housing arrangements
337 and all studies were conducted in the strictest standards of humane animal care under the
338 auspices of the UK Home Office Animals (Scientific Procedures) Act, 1986 and local ethical
339 committee approval.

340

341 Two groups of dams were utilized for this study. Group 1 underwent characterization of
342 changes in placental and umbilical blood velocity and fetal heart development over gestation.
343 A subset of Group 1 dams underwent ultrasound analyses at E14.5 or E17.5 (n = 8 at each time-
344 point). Following imaging, the pregnant dam was euthanized *in situ*, and scanned fetuses
345 excised following identification by corroboration of position with the ultrasound images.
346 Fetuses were fixed and umbilical cords were collected for subsequent myography studies.
347 Placental and fetal tissues were collected from a further subset of dams (n = 8 at each timepoint)
348 for gene expression analysis.

349

350 Group 2 were injected with either saline (Sal) or 20 µg/kg of pravastatin sodium salt (Prav;
351 Cayman Chemical, Cambridge, UK) i.p. daily from E6.5 onwards. At E17.5, a subset

352 underwent ultrasound analyses and placentas were collected for stereological analysis (n = 8)
353 whilst an additional cohort (n = 6 – 8) was generated for placental and fetal gene analysis.

354

355 Umbilical cords were placed in ice-cold Krebs-Henseleit solution prior to subsequent
356 myography studies. For RNA extractions, placentas were dissected rapidly over wet ice and
357 separated into junctional and labyrinth zones before freezing on dry ice. Fetal hearts were
358 dissected and immediately frozen on dry ice. For histological investigations, whole placentas,
359 umbilical cords and fetuses were fixed in formalin and paraffin embedded. Fetal tails were
360 collected in all cases for genotyping and gendertyping by PCR as described (10). However sex
361 was not taken into account in the final analyses due to an insufficient number of each sex for
362 each possible genotype to reach statistical power.

363

364 **High resolution ultrasound analysis**

365 *In vivo* ultrasound assessment was performed using a Vevo 770 ultrasound biomicroscope
366 (Visualsonics; Toronto, Canada) using a RMV707B 30MHz centre frequency transducer.
367 Pregnant mice were scanned as described (26). Fetal-placental units were imaged over a strict
368 20 min time period, with a minimum of three units being analysed in each pregnancy. Blood
369 velocity within the umbilical artery, vein and placenta was measured (46). Fetal hearts were
370 visualized in B-mode and Doppler measurements were undertaken to determine the E/A wave
371 ratio and myocardial performance index (MPI) (26). Images were recorded for offline analysis.

372

373 **Placental and umbilical cord morphology**

374 Placental stereological investigations were conducted as described (10). Umbilical cord
375 morphology was ascertained from four cross-sectional haemotoxylin and eosin stained sections
376 taken from the midline of the umbilical cord, 80 μ m apart. The umbilical artery and vein area
377 and perimeter were calculated by manually tracing the outer smooth muscle outline and lumen
378 perimeter using Nikon NIS Elements Imaging Software v4.10. (Nikon Instruments Inc.,
379 U.S.A.). All measurements were performed by an observer blind to genotype. Treatment and
380 intra-observer error was less than 5%.

381

382 **Cardiac morphology**

383 Serial haemotoxylin and eosin stained sections were assessed using Nikon NIS Elements
384 Imaging Software v4.10. (Nikon Instruments Inc., U.S.A.). Cardiac tissue volume and
385 cardiomyocyte number were determined using stereological investigations as described (47).
386 Ventricle wall thickness was assessed by measuring the thickness of the wall at the point
387 perpendicular from the center of the longest axis of the ventricle.

388

389 **Umbilical vessel myography**

390 The contractile and vasodilator capacity of umbilical vessels was assessed by myography, based
391 on modifications of previously established protocols. Umbilical arteries were carefully
392 dissected, cut into lengths of ~1.5 mm, then mounted on a wire myograph (610M; Danish Myo
393 Technology, Aarhus, Denmark) using 25 µm diameter wire. Vessels were placed at 2 mN
394 pretension, allowed to equilibrate for 30-60 min, before establishing vessel viability with high
395 K⁺ physiological saline solution (K⁺PSS)+noradrenaline (10 µM). Arteries with a contraction
396 of 1 mN or less were excluded from the analysis). Vessels were contracted with increasing
397 doses of thromboxane mimetic (U46619). EC₈₀ concentrations of U46619 were chosen to
398 precontract arteries, before carrying out concentration response curves to the endothelium-
399 dependent vasodilator, acetylcholine (ACh), and the endothelium-independent vasodilator,
400 sodium nitroprusside (SNP). To assess basal endothelial activity, vessels were partially
401 precontracted with EC₅₀ U46619, before addition of the eNOS inhibitor, L_ω-nitro-L-arginine
402 methyl ester (L-NAME; 200 µM), and the cyclooxygenase (COX) inhibitor, indomethacin (10
403 µM). The data from force transducers were processed by a MacLab/4e analogue-digital
404 converter and displayed through Chart software, version 3.4.3 (AD Instruments, Sussex, UK).

405

406 **Quantitative qPCR**

407 Total RNA was extracted from tissue using QIAzol® Lysis reagent (Qiagen Sciences, Victoria,
408 Australia) as per the manufacturer's instructions. Total RNA (1 µg) was reverse transcribed
409 using Mouse Moloney leukemia virus reverse transcriptase (M-MLV) and random primers
410 (Promega, Sydney, Australia). The cDNA was subsequently purified with Ultraclean PCR
411 Cleanup kit (MoBio Laboratories, Inc., Carlsbad, CA).

412

413 Specific mRNA levels were measured by quantitative (q)RT-PCR on the Rotorgene 6000
414 system (Corbett Research, Sydney, Australia) using QuantiTect SYBR Green Mastermix
415 (Qiagen Sciences, Victoria, Australia). Primers for *Vegfa*, peroxisome proliferator-activated
416 receptor gamma (*Pparg*), glucocorticoid-induced leucine zipper (GILZ, for *Tsc22d3*), myosin
417 heavy chain 6 alpha (*Myh6*), sarcoplasmic/endoplasmic reticulum calcium ATPase 2 (*Atp2a2*),
418 natriuretic peptide A (*Nppa*), angiotensin I converting enzyme (*Ace*), collagen, type I, alpha 1
419 (*Col1a1*), collagen, type III, alpha 1 (*Col3a1*), collagen, type IV, alpha 1 (*Col4a1*) were
420 purchased as Qiagen QuantiTect primers with the exception of the internal standards, *Tbp*, *Ppia*
421 and *Sdha*, which were designed using Primer-BLAST (<http://www.ncbi.nlm.nih.gov>). Primer
422 pairs for all genes are listed in Table S4. Standard curves were generated through tenfold serial
423 dilution of purified PCR products for each gene with analysis using Rotorgene 6000 Software.
424 All samples were normalized against *Tbp*, *Sdha* and *Ppia* using the GeNorm algorithm (48).

425

426 **Statistical analysis**

427 All data are expressed as mean \pm SEM, with each litter representing $n = 1$, with no more than
428 1 representative pup per litter analysed. For fetal and placental weights, $n = 14-20$. Fetal sex
429 was noted but was not taken into account in analyses, including fetal weight, as statistical power
430 was insufficient for analysis by gender as well as genotype. For ultrasound ($n = 8$) values were
431 normalized to fetal weight. For heart and umbilical cord morphology and gene expression
432 studies, $n = 6-8$. Two-way ANOVA followed by Tukey's *post hoc* test or one-way ANOVA
433 followed by Tukey's *post hoc* test were used as appropriate. $p < 0.05$ was accepted as statistically
434 significant.

435

436

437 **Acknowledgements**

438 The funding sources of this study were Wellcome Trust project grant (WT079009) and EU
439 FP7 collaborative grant Developmental origins of healthy and unhealthy ageing (DORIAN,
440 grant n. 278603) to MCH and JRS, and The Raine Medical Research Priming Grant (CSW).
441 ER-Z was funded by a studentship from the British Heart Foundation.

442 **References**

443

- 444 1. Godfrey KM & Barker DJ (2001) Fetal programming and adult health. *Public health*
 445 *nutrition* 4(2B):611-624.
- 446 2. Fowden AL & Forhead AJ (2015) Glucocorticoids as regulatory signals during
 447 intrauterine development. *Exp Physiol*.
- 448 3. Wyrwoll CS, Mark PJ, Mori TA, Puddey IB, & Waddell BJ (2006) Prevention of
 449 programmed hyperleptinemia and hypertension by postnatal dietary omega-3 fatty
 450 acids. *Endocrinology* 147(1):599-606.
- 451 4. Wyrwoll CS, Mark PJ, Mori TA, & Waddell BJ (2008) Developmental programming
 452 of adult hyperinsulinemia, increased proinflammatory cytokine production, and altered
 453 skeletal muscle expression of SLC2A4 (GLUT4) and uncoupling protein 3. *J*
 454 *Endocrinol* 198(3):571-579.
- 455 5. Benediktsson R, Lindsay RS, Noble J, Seckl JR, & Edwards CR (1993) Glucocorticoid
 456 exposure in utero: new model for adult hypertension. *Lancet* 341(8841):339-341.
- 457 6. Lindsay RS, Lindsay RM, Edwards CR, & Seckl JR (1996) Inhibition of 11-beta-
 458 hydroxysteroid dehydrogenase in pregnant rats and the programming of blood pressure
 459 in the offspring. *Hypertension* 27(6):1200-1204.
- 460 7. Nyirenda MJ, Lindsay RS, Kenyon CJ, Burchell A, & Seckl JR (1998) Glucocorticoid
 461 exposure in late gestation permanently programs rat hepatic phosphoenolpyruvate
 462 carboxykinase and glucocorticoid receptor expression and causes glucose intolerance
 463 in adult offspring. *J Clin Invest* 101(10):2174-2181.
- 464 8. O'Regan D, Kenyon CJ, Seckl JR, & Holmes MC (2004) Glucocorticoid exposure in
 465 late gestation in the rat permanently programs gender-specific differences in adult
 466 cardiovascular and metabolic physiology. *Am J Physiol Endocrinol Metab*
 467 287(5):E863-870.
- 468 9. Hewitt DP, Mark PJ, & Waddell BJ (2006) Glucocorticoids prevent the normal
 469 increase in placental vascular endothelial growth factor expression and placental
 470 vascularity during late pregnancy in the rat. *Endocrinology* 147(12):5568-5574.
- 471 10. Wyrwoll CS, Seckl JR, & Holmes MC (2009) Altered placental function of 11beta-
 472 hydroxysteroid dehydrogenase 2 knockout mice. *Endocrinology* 150(3):1287-1293.
- 473 11. Brown RW, *et al.* (1996) The ontogeny of 11 beta-hydroxysteroid dehydrogenase type
 474 2 and mineralocorticoid receptor gene expression reveal intricate control of
 475 glucocorticoid action in development. *Endocrinology* 137(2):794-797.
- 476 12. Burton PJ, Smith RE, Krozowski ZS, & Waddell BJ (1996) Zonal distribution of 11
 477 beta-hydroxysteroid dehydrogenase types 1 and 2 messenger ribonucleic acid
 478 expression in the rat placenta and decidua during late pregnancy. *Biol Reprod*
 479 55(5):1023-1028.
- 480 13. Mairesse J, *et al.* (2007) Maternal stress alters endocrine function of the fetoplacental
 481 unit in rats. *Am J Physiol Endocrinol Metab* 292(6):E1526-1533.
- 482 14. O'Donnell KJ, *et al.* (2012) Maternal prenatal anxiety and downregulation of placental
 483 11beta-HSD2. *Psychoneuroendocrinology* 37(6):818-826.
- 484 15. Cottrell EC, Seckl JR, Holmes MC, & Wyrwoll CS (2013) Foetal and placental 11beta-
 485 HSD2: a hub for developmental programming. *Acta Physiol (Oxf)*.
- 486 16. Vaughan OR, Sferruzzi-Perri AN, Coan PM, & Fowden AL (2013) Adaptations in
 487 placental phenotype depend on route and timing of maternal dexamethasone
 488 administration in mice. *Biol Reprod* 89(4):80.
- 489 17. Barker DJ, *et al.* (2012) The placental origins of sudden cardiac death. *Int J Epidemiol*
 490 41(5):1394-1399.
- 491 18. Thornburg KL, O'Tierney PF, & Louey S (2010) Review: The placenta is a
 492 programming agent for cardiovascular disease. *Placenta* 31 Suppl:S54-59.
- 493 19. Kiserud T, Ebbing C, Kessler J, & Rasmussen S (2006) Fetal cardiac output,
 494 distribution to the placenta and impact of placental compromise. *Ultrasound Obstet*
 495 *Gynecol* 28(2):126-136.

- 496 20. Shaut CA, Keene DR, Sorensen LK, Li DY, & Stadler HS (2008) HOXA13 Is essential
497 for placental vascular patterning and labyrinth endothelial specification. *PLoS Genet*
498 4(5):e1000073.
- 499 21. Adams RH, *et al.* (2000) Essential role of p38alpha MAP kinase in placental but not
500 embryonic cardiovascular development. *Mol Cell* 6(1):109-116.
- 501 22. Barak Y, *et al.* (1999) PPAR gamma is required for placental, cardiac, and adipose
502 tissue development. *Mol Cell* 4(4):585-595.
- 503 23. Ahmed A, Singh J, Khan Y, Seshan SV, & Girardi G (2010) A new mouse model to
504 explore therapies for preeclampsia. *PLoS ONE* 5(10):e13663.
- 505 24. Michelsohn AM & Anderson DJ (1992) Changes in competence determine the timing
506 of two sequential glucocorticoid effects on sympathoadrenal progenitors. *Neuron*
507 8(3):589-604.
- 508 25. Corrigan N, Brazil DP, & Auliffe FM (2010) High-frequency ultrasound assessment
509 of the murine heart from embryo through to juvenile. *Reprod Sci* 17(2):147-157.
- 510 26. Rog-Zielinska EA, *et al.* (2013) Glucocorticoid receptor is required for foetal heart
511 maturation. *Hum Mol Genet* 22(16):3269-3282.
- 512 27. Rubattu S & Volpe M (2001) The atrial natriuretic peptide: a changing view. *J*
513 *Hypertens* 19(11):1923-1931.
- 514 28. Lu B, *et al.* (2012) Identification of hypertrophy- and heart failure-associated genes by
515 combining in vitro and in vivo models. *Physiological genomics* 44(8):443-454.
- 516 29. Jozkowicz A, Dulak J, Piatkowska E, Placha W, & Dembinska-Kiec A (2000) Ligands
517 of peroxisome proliferator-activated receptor-gamma increase the generation of
518 vascular endothelial growth factor in vascular smooth muscle cells and in
519 macrophages. *Acta biochimica Polonica* 47(4):1147-1157.
- 520 30. Bishop JE & Laurent GJ (1995) Collagen turnover and its regulation in the normal and
521 hypertrophying heart. *European heart journal* 16 Suppl C:38-44.
- 522 31. Kotelevtsev Y, *et al.* (1999) Hypertension in mice lacking 11beta-hydroxysteroid
523 dehydrogenase type 2. *J Clin Invest* 103(5):683-689.
- 524 32. Barker DJ, Thornburg KL, Osmond C, Kajantie E, & Eriksson JG (2010) The surface
525 area of the placenta and hypertension in the offspring in later life. *Int J Dev Biol* 54(2-
526 3):525-530.
- 527 33. Eriksson JG, Kajantie E, Thornburg KL, Osmond C, & Barker DJ (2011) Mother's
528 body size and placental size predict coronary heart disease in men. *European heart*
529 *journal* 32(18):2297-2303.
- 530 34. Thornburg KL, O'Tierney PF, & Louey S (2010) The Placenta is a Programming Agent
531 for Cardiovascular Disease. *Placenta* 31:S54-S59.
- 532 35. Okada Y, *et al.* (2007) Complementation of placental defects and embryonic lethality
533 by trophoblast-specific lentiviral gene transfer. *Nat Biotechnol* 25(2):233-237.
- 534 36. Giussani DA, *et al.* (2012) Developmental programming of cardiovascular dysfunction
535 by prenatal hypoxia and oxidative stress. *PLoS One* 7(2):e31017.
- 536 37. Richter HG, *et al.* (2012) Ascorbate prevents placental oxidative stress and enhances
537 birth weight in hypoxic pregnancy in rats. *J Physiol* 590(Pt 6):1377-1387.
- 538 38. Kane AD, Herrera EA, Hansell JA, & Giussani DA (2012) Statin treatment depresses
539 the fetal defence to acute hypoxia via increasing nitric oxide bioavailability. *J Physiol*
540 590(Pt 2):323-334.
- 541 39. Kumasawa K, *et al.* (Pravastatin induces placental growth factor (PGF) and ameliorates
542 preeclampsia in a mouse model. *Proc Natl Acad Sci U S A* 108(4):1451-1455.
- 543 40. Ramma W & Ahmed A (2014) Therapeutic potential of statins and the induction of
544 heme oxygenase-1 in preeclampsia. *Journal of reproductive immunology* 101-102:153-
545 160.
- 546 41. Saad AF, *et al.* (2014) Effects of pravastatin on angiogenic and placental hypoxic
547 imbalance in a mouse model of preeclampsia. *Reprod Sci* 21(1):138-145.
- 548 42. Forbes K, *et al.* (2015) Statins inhibit insulin-like growth factor action in first trimester
549 placenta by altering insulin-like growth factor 1 receptor glycosylation. *Mol Hum*
550 *Reprod* 21(1):105-114.

551 43. Zarek J, *et al.* (2013) The transfer of pravastatin in the dually perfused human placenta.
552 *Placenta* 34(8):719-721.

553 44. Nanovskaya TN, *et al.* (2013) Transplacental transfer and distribution of pravastatin.
554 *Am J Obstet Gynecol* 209(4):373 e371-375.

555 45. Holmes MC, *et al.* (2006) The mother or the fetus? 11beta-hydroxysteroid
556 dehydrogenase type 2 null mice provide evidence for direct fetal programming of
557 behavior by endogenous glucocorticoids. *J Neurosci* 26(14):3840-3844.

558 46. Mu J & Adamson SL (2006) Developmental changes in hemodynamics of uterine
559 artery, utero- and umbilicoplacental, and vitelline circulations in mouse throughout
560 gestation. *Am J Physiol Heart Circ Physiol* 291(3):H1421-1428.

561 47. Corstius HB, *et al.* (2005) Effect of intrauterine growth restriction on the number of
562 cardiomyocytes in rat hearts. *Pediatr Res* 57(6):796-800.

563 48. Vandesompele J, *et al.* (2002) Accurate normalization of real-time quantitative RT-
564 PCR data by geometric averaging of multiple internal control genes. *Genome biology*
565 3(7):RESEARCH0034.

566

567

568 **Tables**

569 **Table 1:** E17.5 fetal and placental weights of *Hsd11b2*^{+/+}, *Hsd11b2*^{+/-} and *Hsd11b2*^{-/-} fetuses
 570 from saline (Sal) or pravastatin-treated (Prav) dams.

571

	Sal (n=28)			Prav (n=32)		
	+/+	+/-	-/-	+/+	+/-	-/-
Fetal weight (g)	0.81±0.02 ^a	0.83±0.021 ^a	0.73±0.03 ^c	0.87±0.01 ^d	0.85±0.01 ^{bd}	0.81±0.01 ^a
Placental weight (g)	0.09±0.03 ^a	0.09±0.02 ^a	0.08±0.03 ^a	0.1±0.03 ^b	0.1±0.03 ^b	0.1±0.04 ^b

572 Values are the mean ± SEM. Values without common notation differ significantly (p<0.05,
 573 two-way ANOVA, Tukey's *post hoc* test). Sal, Saline-treated dams; Prav, Pravastatin-treated
 574 dams.

575

576

577

578

579

580

581 **Figure Legends**

582

583 **Figure 1:** Umbilical vein velocity (A), umbilical artery resistance index (B) and fetal cardiac
584 E/A wave ratio (C) in *Hsd11b2*^{+/+}, *Hsd11b2*^{+/-} and *Hsd11b2*^{-/-} fetuses at E14.5 and E17.5. Values
585 were normalized for fetal weight and are the mean \pm SEM (n = 8 per group). Columns without
586 common notation differ significantly (p<0.05, two-way ANOVA, Tukey's *post hoc* test).

587

588 **Figure 2:** Contractile and vasodilator function of umbilical arteries. (A) H&E stained cross-
589 section of the umbilical cord. Scale bar = 100 μ m. Inset, higher magnification of the umbilical
590 artery used for myography studies. Arrows indicate the presence of endothelial cell nuclei on
591 the luminal surface of the artery. (B) Maximal contraction of arteries to high potassium
592 physiological saline solution containing noradrenaline (K⁺PSS+NA) in animal with disrupted
593 *Hsd11b2* alleles. (C) Maximum vasodilator response to the thromboxane mimetic U46619 in
594 umbilical arteries from *Hsd11b2*^{-/-} fetuses (*P<0.05, unpaired t-test of K_{max}). (D) Contractile
595 response to inhibition of basal endothelium-dependent relaxation in response to L_ω-nitro-L-
596 arginine methyl ester (L-NAME) and indomethacin (**P<0.01, unpaired t-test). (E)
597 Vasodilator response to sodium nitroprusside (SNP). For B, C & E, data shown are the mean \pm
598 SEM (n=6, 20, 9 for *Hsd11b2*^{+/+}, *Hsd11b2*^{+/-}, *Hsd11b2*^{-/-}, respectively). For D, data shown are
599 the mean \pm SEM (n=5, 11, 8 for *Hsd11b2*^{+/+}, *Hsd11b2*^{+/-}, *Hsd11b2*^{-/-}, respectively).

600

601 **Figure 3:** Relative levels of (A) *Tsc22d3*, (B) *Myh6*, (C) *Atp2a2* and (D) *Nppa* mRNA in hearts
602 of *Hsd11b2*^{+/+}, *Hsd11b2*^{+/-} and *Hsd11b2*^{-/-} fetuses at E14.5 and E17.5. Values are means \pm SEM
603 (n = 6-8 per group). Columns without common notation differ significantly (p<0.05, two-way
604 ANOVA, Tukey's *post hoc* test).

605

606 **Figure 4:** Placental gene expression and morphology in control and pravastatin treated
607 *Hsd11b2*^{+/+}, *Hsd11b2*^{+/-} and *Hsd11b2*^{-/-} fetuses. (A) Relative labyrinth zone *Vegfa* mRNA
608 expression and (B) *Pparg* mRNA expression, (C) labyrinth zone (LZ) fraction and (D) fetal
609 capillary (FC) volume. Values are the mean \pm SEM (n = 6-8 per group). Columns without
610 common notation differ significantly (p<0.05, two-way ANOVA, Tukey's *post hoc* test). Sal,
611 Saline-treated; Prav, Pravastatin-treated, LZ, labyrinth zone; FC, fetal capillaries.

612

613 **Figure 5:** Umbilical vein velocity (A), umbilical artery resistance index (B) and fetal cardiac
614 E/A wave ratio (C) in saline and pravastatin treated *Hsd11b2*^{+/+}, *Hsd11b2*^{+/-} and *Hsd11b2*^{-/-}
615 fetuses. Values were normalized for fetal weight and are the mean \pm SEM (n = 8 per group).
616 Columns without common notation differ significantly (p<0.05, two-way ANOVA, Tukey's
617 *post hoc* test). Sal, Saline-treated; Prav, Pravastatin-treated.

618

619 **Figure 6:** Fetal cardiac gene expression in control and pravastatin treated *Hsd11b2*^{+/+},
620 *Hsd11b2*^{+/-} and *Hsd11b2*^{-/-} fetuses. Relative levels of (A) *Tsc22d3*, (B) *Myh6*, (C) *Atp2a2*, (D)
621 *Nppa*, (E) *Ace*, (F) *Colla1*, (G) *Col3a1* and (H) *Col4a1*. Values are the mean \pm SEM (n = 6-8
622 per group). Columns without common notation differ significantly (p<0.05, two-way ANOVA,
623 Tukey's *post hoc* test). In the case of *Col4a1* *p<0.05, t-test of corresponding genotype between
624 treatments. Sal, Saline-treated; Prav, Pravastatin-treated.

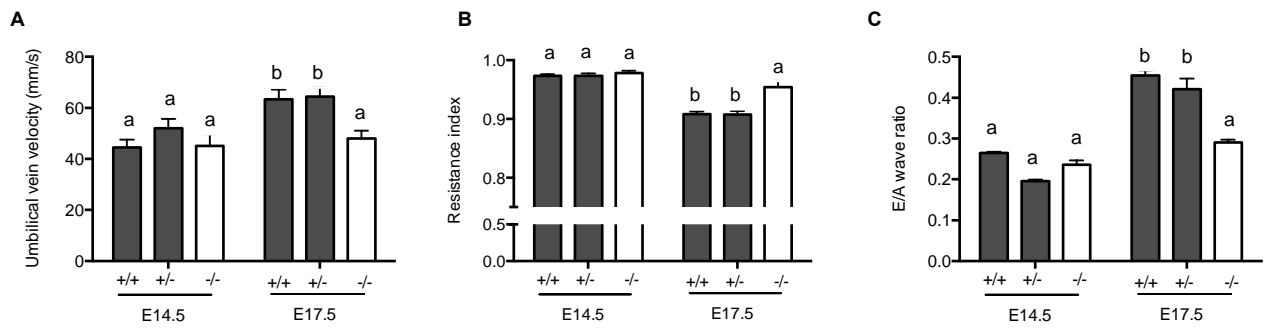
625

626

627

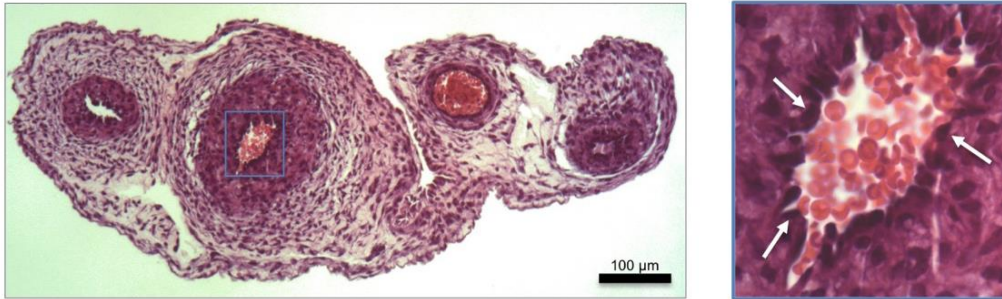
628

629 **Figure 1**

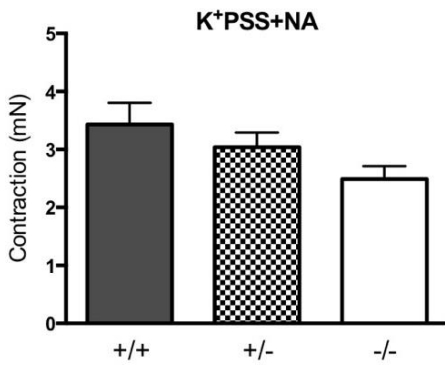


630

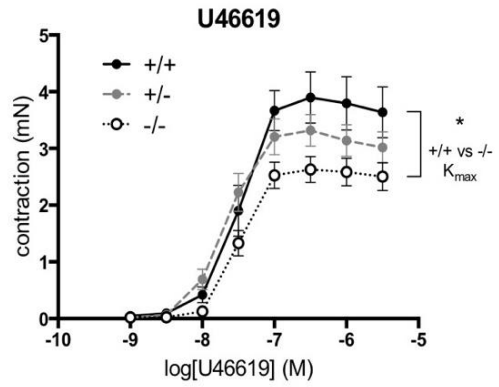
A



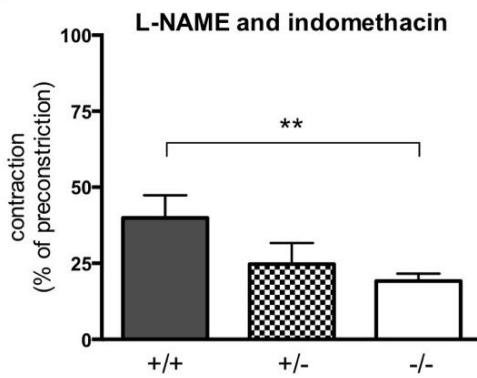
B



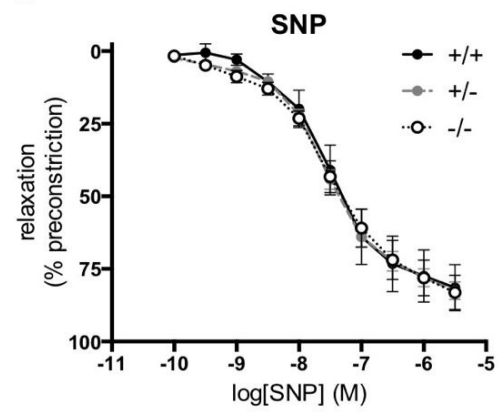
C



D

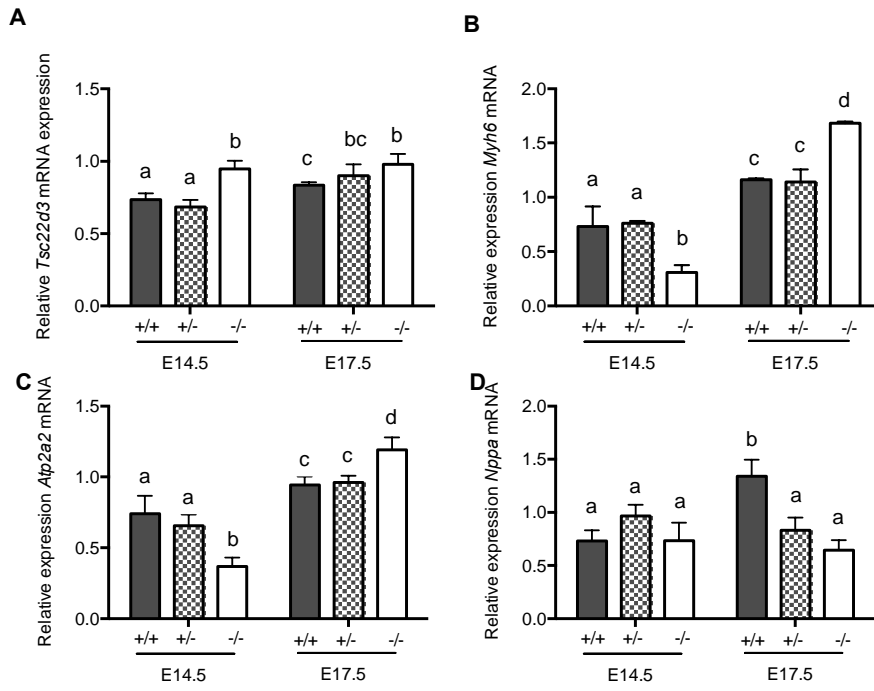


E



632

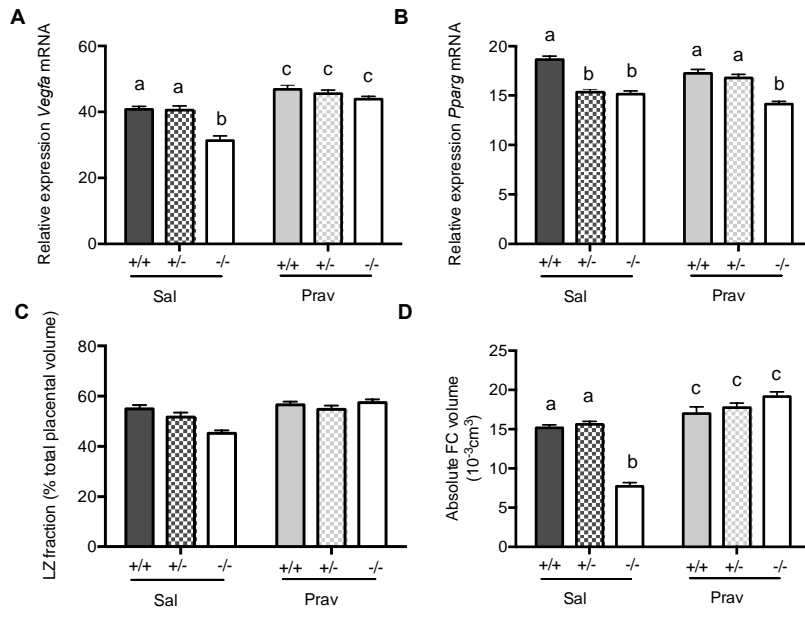
633



635

636

637 **Figure 4**



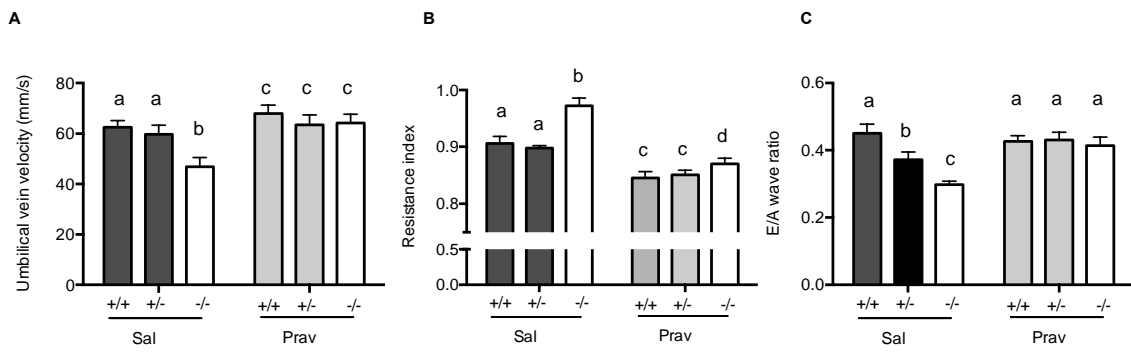
638

639

640

641

642 **Figure 5**



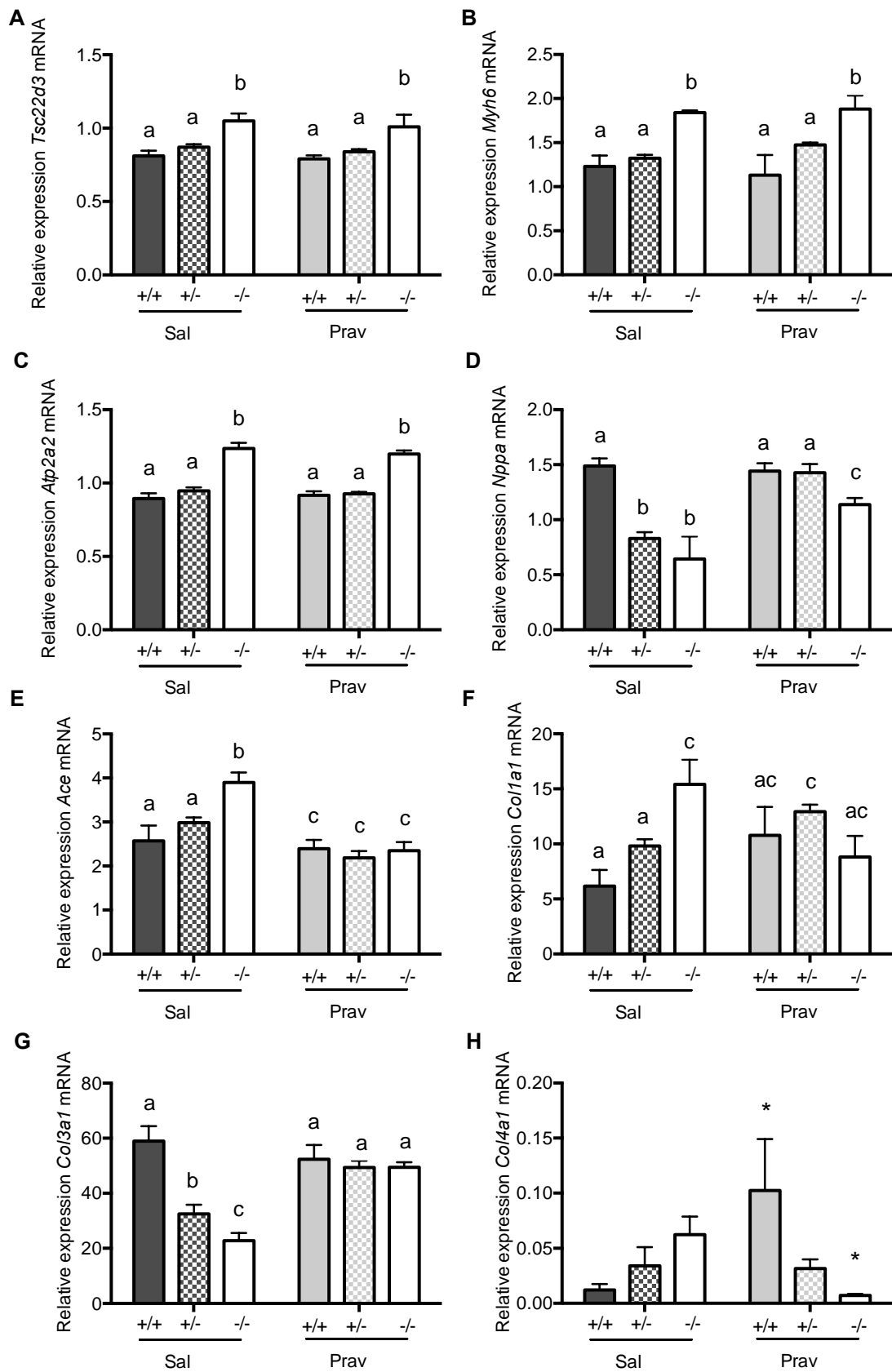
643

644

645

646

647 **Figure 6**



648

649

650

651 Supporting Information

652

653 Table S1: Myocardial performance index of *Hsd11b2*^{+/+}, *Hsd11b2*^{+/-} and *Hsd11b2*^{-/-} fetuses at
 654 E14.5 and E17.5. Values without common notation differ significantly.
 655

	E14.5			E17.5		
	<i>Hsd11b2</i> ^{+/+}	<i>Hsd11b2</i> ^{+/-}	<i>Hsd11b2</i> ^{-/-}	<i>Hsd11b2</i> ^{+/+}	<i>Hsd11b2</i> ^{+/-}	<i>Hsd11b2</i> ^{-/-}
MPI	0.75±0.05 ^a	0.75±0.02 ^a	0.72±0.03 ^a	0.63±0.03 ^b	0.64±0.02 ^b	0.65±0.03 ^b
IVCT (ms)	22±0.3 ^a	23.4±0.1 ^a	22.8±0.2 ^a	18.1±0.2 ^b	16.9±0.4 ^b	19.6±1 ^b
ET (ms)	101.4±5	97.3±3	105.6±5	105.3±2	98.6±5	102.6±4
IVRT (ms)	26.1±3 ^a	24.8±2 ^a	25.9±3 ^a	22.4±3 ^b	20.1±1 ^b	21.7±0.5 ^b
EDD (mm/s ²)	1542±481 ^a	1329±312 ^a	1376±548 ^a	3128±682 ^b	3308±384 ^b	1365±445 ^a
EF (%)	73.8±3.5 ^a	76.2±2 ^a	71.8±1.4 ^a	85.2±2.1 ^b	81.3±1.9 ^b	82.6±1.5 ^b

656 Values are the mean ± SEM. MPI, myocardial performance index; IVCT, isovolumetric
 657 contraction time; ET, ejection time; IVRT, isovolumetric relaxation time; EDD, early
 658 diastolic deceleration; EF, ejection fraction
 659

660

661

661 **Table S2:** Lumen and vessel wall area of umbilical arteries and vein from *Hsd11b2*^{+/+} and
 662 *Hsd11b2*^{-/-} fetuses.

	Umbilical artery		Umbilical vein	
	<i>Hsd11b2</i> ^{+/+}	<i>Hsd11b2</i> ^{-/-}	<i>Hsd11b2</i> ^{+/+}	<i>Hsd11b2</i> ^{-/-}
Lumen area (µm ²)	4211±1265	3624±986	36211±8246	29425±6937
Vessel wall area (µm ²)	32646±1324	28436±2534	24328±879	18656±2289

663 Values are the mean ± SEM

664

665 **Table S3:** Pravastatin treatment does not affect maternal body weight, organ weight or litter
 666 size.

	Sal (n=28)	Prav (n=32)
E17.5 maternal weight (g)	31.7±1.7	32.0±1.9
Brain weight (g)	0.46±0.01	0.47±0.01
Liver weight (g)	1.63±0.07	1.8±0.06
Heart weight (g)	0.15±0.01	0.18±0.01
Left kidney weight (g)	0.15±0.01	0.15±0.01
Litter size	8.1±0.8	9.1±0.5

667 Values are the mean ± SEM. Sal, Saline-treated dams; Prav, Pravastatin-treated dams.

668

669

670 **Table S4: PCR conditions**

Gene	Qiagen QuantiTect name or Primer sequence
<i>Vegfa</i>	QT00160769
<i>Pparg</i>	QT00100296
<i>Tsc22d3</i>	QT01552005
<i>Nr3c1</i>	QT00160349
<i>Nr3c2</i>	QT00312305
<i>Myh6</i>	QT00160902
<i>Atp2a2</i>	QT00149121
<i>Nppa</i>	QT00250922
<i>Ace</i>	QT00100135
<i>Col1a1</i>	QT 00162204
<i>Col3a1</i>	QT 01055516
<i>Col4a1</i>	QT 00287392
<i>Col5a1</i>	QT 01055474
<i>Sdha</i>	F, 5'-TGGGGCGACTCGTGGCTTTC- 3' R, 5'-CCCCGCCTGCACCTACAACC- 3'
<i>Ppia</i>	F, 5'-AGCATACAGGTCCTGGCATC- 3' R, 5'-TTCACCTTCCCAAAGACCAC- 3'
<i>Tbp</i>	F 5' GGGAGAATCATGGACCAGAA '3 R 5' CCGTAAGGCATCATTGGACT '3

671 Qiagen QuantiTect primer name and primer sequences for analysis and reference genes. F,
 672 forward; R, reverse.

673

674

675

676 **Table S5:** Pravastatin treatment does not alter overall cardiac volume, ventricular lumen
 677 volume or the ratio of ventricular wall thickness to lumen volume of *Hsd11b2*^{+/+}, *Hsd11b2*^{+/-},
 678 and *Hsd11b2*^{-/-} fetuses.

	Sal			Prav		
	<i>Hsd11b2</i> ^{+/+}	<i>Hsd11b2</i> ^{+/-}	<i>Hsd11b2</i> ^{-/-}	<i>Hsd11b2</i> ^{+/+}	<i>Hsd11b2</i> ^{+/-}	<i>Hsd11b2</i> ^{-/-}
Cardiac volume (mm ³)	3.8±0.4	3.6±0.3	3.5±0.2	3.7±0.2	3.8±0.3	3.6±0.2
LV lumen volume (mm ³)	0.87±0.16	0.6±0.08	1.07±0.2	1.15±0.1	0.87±0.07	0.76±0.12
LV wall thickness: Lumen volume	0.46±0.03	0.45±0.02	0.49±0.05	0.44±0.04	0.43±0.05	0.45±0.02
RV lumen volume (mm ³)	0.89±0.06	0.58±0.18	0.88±0.13	1.04±0.2	0.62±0.1	0.79 ±0.1
RV wall thickness: Lumen volume	0.42±0.05	0.39±0.04	0.44±0.06	0.43±0.02	0.41±0.03	0.41±0.04

679 Values are the mean ± SEM. Sal, Saline-treated; Prav, Pravastatin-treated; LV, left ventricle;

680 RV, right ventricle

681

682

683 **Figure S1:** Acetylcholine (ACh) did not relax umbilical arteries. There were no significant
684 differences between genotypes. Symbols shown are mean±SEM (n=6, 12 & 9 for *Hsd11b2*^{+/+},
685 *Hsd11b2*^{+/-}, *Hsd11b2*^{-/-}, respectively).

686

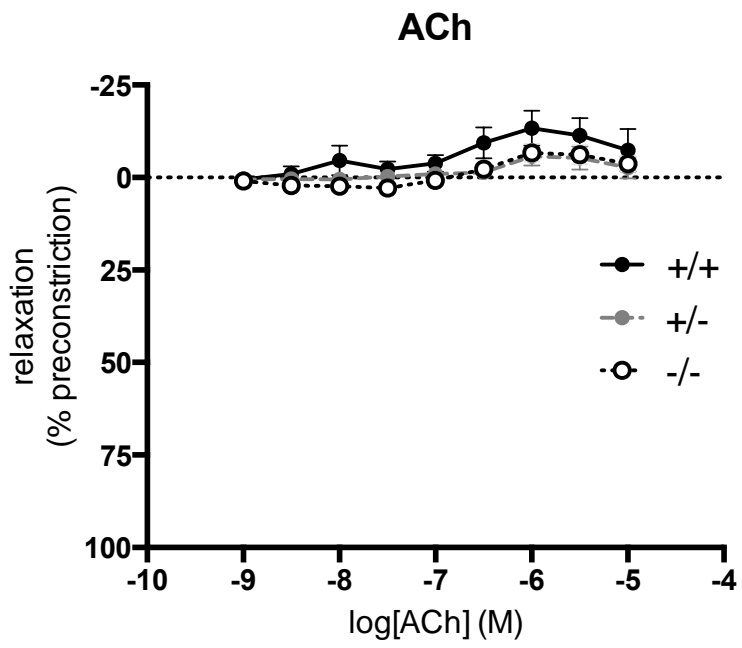
687

688

689

690 **Figure S1**

691



692